Electronic Supplementary Material (ESI) for ChemComm.

Surface induced dissociation as a tool to study membrane protein complexes

Sophie R. Harvey[1,2], Yang Liu[3], Wen Liu[3], Vicki H. Wysocki[1,*] and Arthur Laganowsky[3,4,*].

1. The Department of Chemistry and Biochemistry, The Ohio State University, 460 W 12th Avenue, Columbus, Ohio, 43210, USA.

2. School of Chemistry, Manchester Institute of Biotechnology, University of Manchester, Manchester, M1 7DN, UK.

3. Institute of Biosciences and Technology, Texas A&M Health Science Center, Houston, Texas, 77030, USA.

4. Department of Chemistry, Texas A&M University, College Station, Texas, 77843, USA.

Materials and methods

Sample preparation

AqpZ and AmtB samples were expressed and purified as previously reported[1]. Phospholipids were purchased from Avanti (Avanti Polar Lipids Inc, Alabama, USA) and prepared at stock concentrations of 10 mM in water + 0.5 % β-mercaptoethanol (bME) and 2x critical micelle concentration (CMC) of the detergent tetraethylene glycol monooctyl ether (C_8E_4). For MS analysis the protein samples were buffer exchanged into 200 mM ammonium acetate plus 2xCMC of C_8E_4 using BioRad microspin 6 buffer exchange columns. For studies of the *apo* protein complexes, samples were prepared at 15 µM complex concentration. For AmtB lipid binding studies, samples were prepared at 10 µM protein complex concentration plus 40 µM lipid concentration. For AqpZ lipid binding studies, samples were prepared at 10 µM protein complex concentration plus 50 µM lipid concentration.

Ion mobility Mass Spectrometry and Surface induced dissociation

All mass spectrometry, ion mobility-mass spectrometry, and surface induced dissociation (SID) studies were performed on a Synapt G2 (Waters, Milford, UK). The instrument was modified, as previously described[2], to enable SID experiments to be performed. In brief, the Trap T-wave cell was truncated enabling an SID device containing a fluorocarbon coated gold surface to be installed before the ion mobility cell and the potentials on the lenses in the device were supplied via an external power supply (Ardara Technologies, Ardara, PA). For MS experiments, the lenses were tuned to allow the ion beam to pass through the device without hitting the surface, while in SID mode the ion beam is directed up towards the surface, colliding with the fluorocarbon self-assembled monolayer and causing dissociation.

Typical experimental parameters were as follows; capillary voltage of 1.2-1.4 kV, a sampling cone of 90 V, source temperature of 120 °C, trap collision energy of 5 V. Initial experiments were also performed using a sampling cone of 90 V, source temperature of 20 °C, trap collision energy of 60 V; however, it was determined that using a higher source temperature and lower trap CID energy was advantageous as it allowed for clean-up before the quadrupole and therefore clean *m/z* isolation. Gas flows in the trap, helium cell and ion mobility cell were 4, 120, and 60 mL/min respectively. The cone voltage and source temperature are set higher than in typical native MS experiments for soluble proteins, to aid in detergent removal from the protein complex.

Experimental collisional cross sections were determined using a calibration procedure, with β-lactoglobulin, avidin, concanavilin A, and serum amyloid P component as standards[3]. In all cases, a trap wave velocity of 160 m/s and height of 4 V, ion mobility wave velocity of 300 m/s and height of 20 V, and a transfer wave velocity of 50 m/s and a height of 4 V were used. For the calibration complexes a source temperature of 20 °C and a cone voltage of 20 V was used. Theoretical collisional cross sections were determined from the solved structures PDB 1RC2 for AqpZ and PDB 1U7G for AmtB, using MOBCAL with the scaled projection approximation (PA) approach. Subcomplex CCS were determined by clipping the subunits from the solved structures, for the AqpZ trimer the structure was rearranged into a collapsed form using PyMol.

Supplementary Tables

Table S1: CCS (Å^2) for trimeric AmtB determined through the calibration procedure using travelling wave IM. Tetramer was liberated from the detergent micelle either with a low source temperature (20 °C), high cone voltage (90 V) and high Trap CID voltage (60 V) or a high source temperature (120 °C), high cone voltage (90 V) and low CID voltage (5 V). In either case the CCS values generated for the intact trimer are similar. Under both experimental conditions, two conformations are observed for the highest charge state of the AmtB trimer, with the larger CCS being attributed to activation and partial unfolding.

Species	**Source 20 °C, Cone 90 V, CID 60 V**	**Source 120 °C, Cone 90 V, CID 5 V**
$[AmtB_3+19H]^{19+}$		6142 ± 40 Å^2, 6580 ± 59 Å^2
$[AmtB_3+18H]^{18+}$	6021 ± 38 Å^2, 6515 ± 26 Å^2	6046 ± 9 Å^2
$[AmtB_3+17H]^{17+}$	5954 ± 29 Å^2	5985 ± 4 Å^2
$[AmtB_3+16H]^{16+}$	5896 ± 26 Å^2	5941 ± 13 Å^2
$[AmtB_3+15H]^{15+}$	5829 ± 29 Å^2	5899 ± 36 Å^2

Table S2: CCS (Å^2) for tetrameric AqpZ determined through the calibration procedure using travelling wave IM. Tetramer was liberated from the detergent micelle either with a low source temperature (20 °C), high cone voltage (90 V) and high Trap CID voltage (60 V) or a high source temperature (120 °C), high cone voltage (90 V) and low CID voltage (5 V). In either case the CCS generated for the intact tetramer are similar.

Species	**Source 20 °C, Cone 90 V, CID 60 V**	**Source 120 °C, Cone 90 V, CID 5 V**
$[AqpZ_4+16H]^{16+}$	-	5110 ± 26 Å^2
$[AqpZ_4+15H]^{15+}$	5083 ± 22 Å^2	5059 ± 13 Å^2
$[AqpZ_4+14H]^{14+}$	5001 ± 14 Å^2	5018 ± 7 Å^2
$[AqpZ_4+13H]^{13+}$	4940 ± 20 Å^2	4967 ± 5 Å^2
$[AqpZ_4+12H]^{12+}$	4872 ± 19 Å^2	4900 ± 13 Å^2

Supplementary Figures

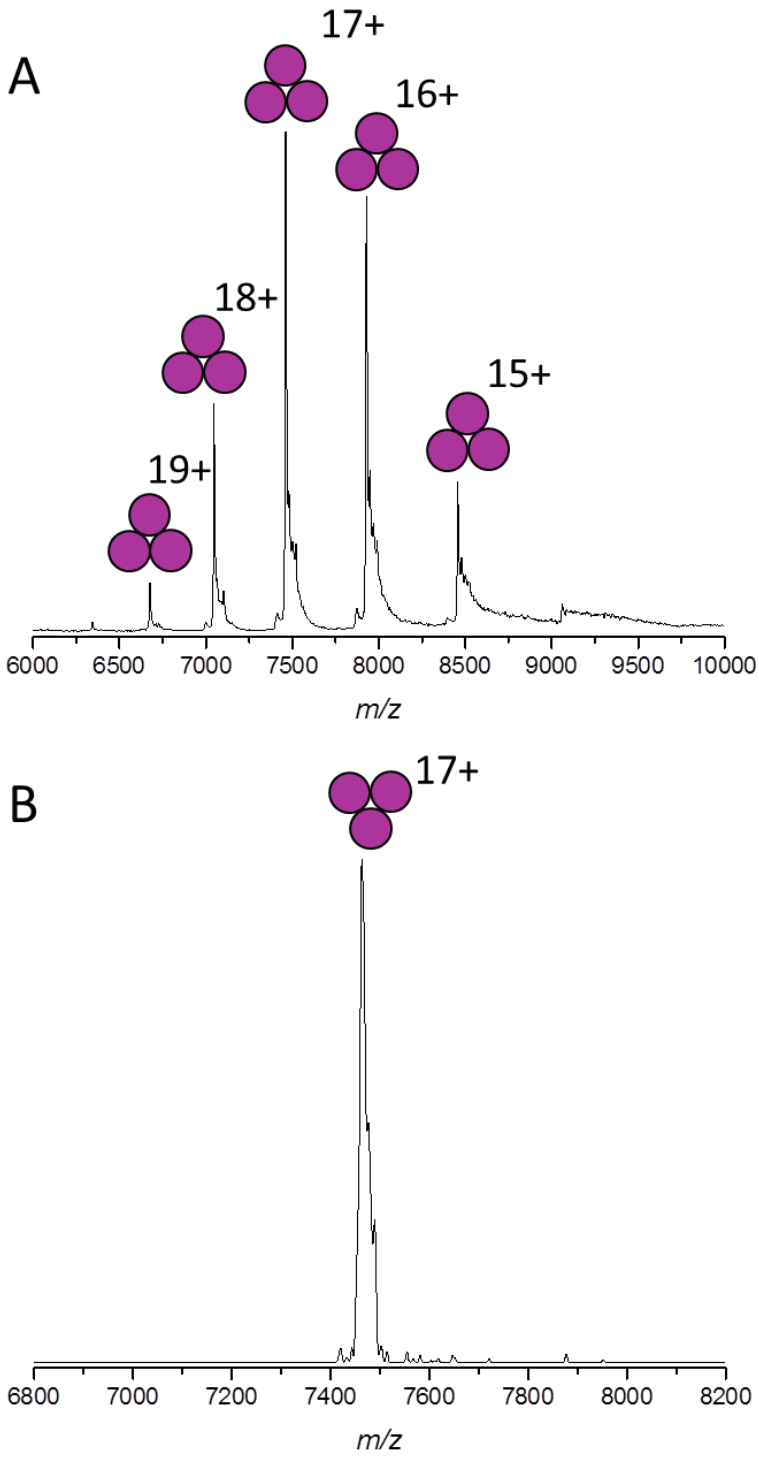

Figure S1: A) Full mass spectrum shown of AmtB, no mass selection. B) Mass spectrum following quadrupole selection of the 17+ trimeric AmtB.

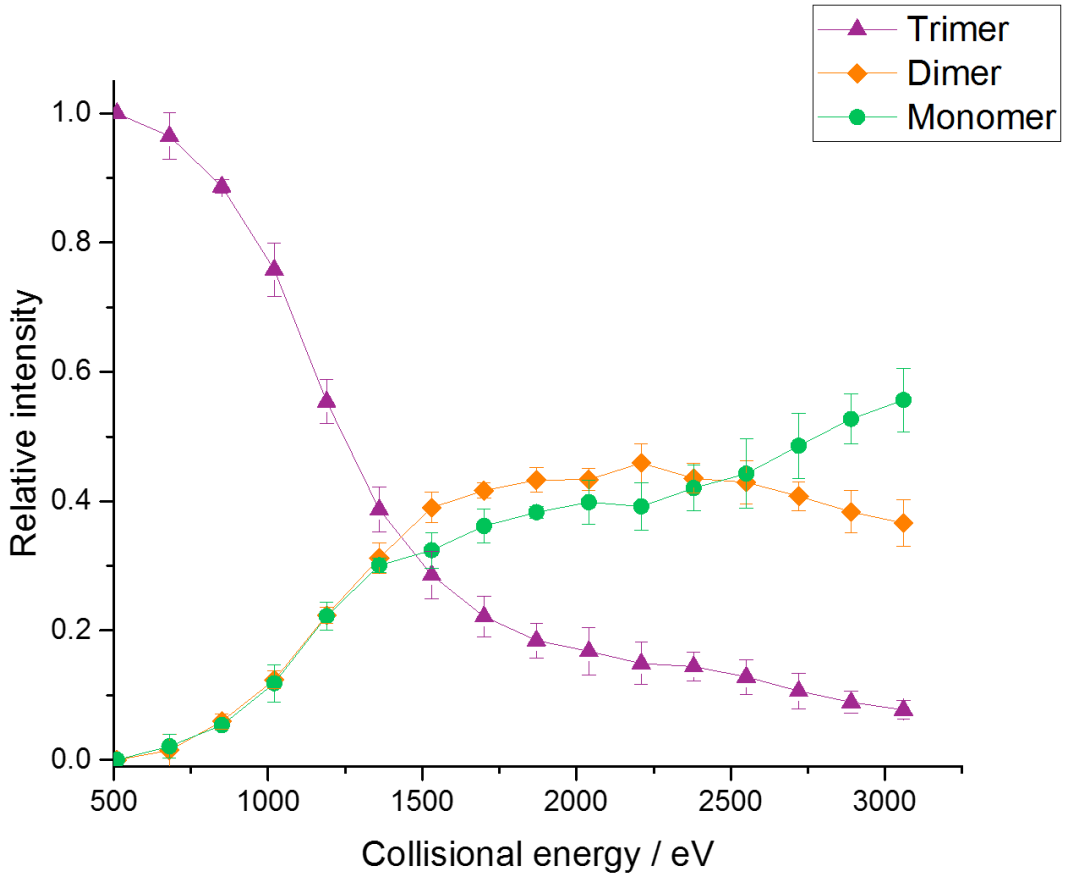

Figure S2: Energy resolved mass spectrometry plot showing the intensity of products produced from the 17+ AmtB trimer, as a function of SID energy. Relative intensities are the average of three repeats and error bars represent the standard deviation (*n* = 3).

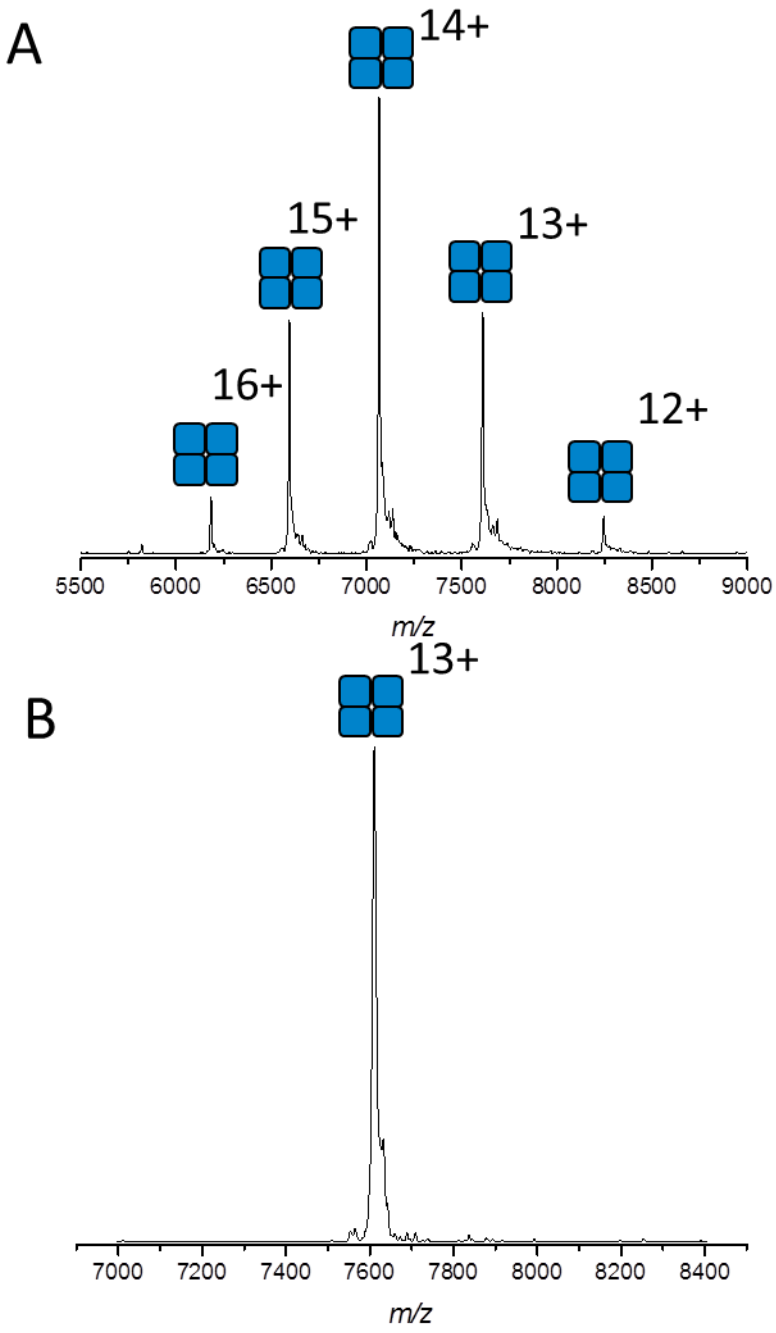

Figure S3: A) Full mass spectrum shown of AqpZ, no mass selection. B) Mass spectrum following quadrupole selection of the 13+ tetrameric AqpZ.

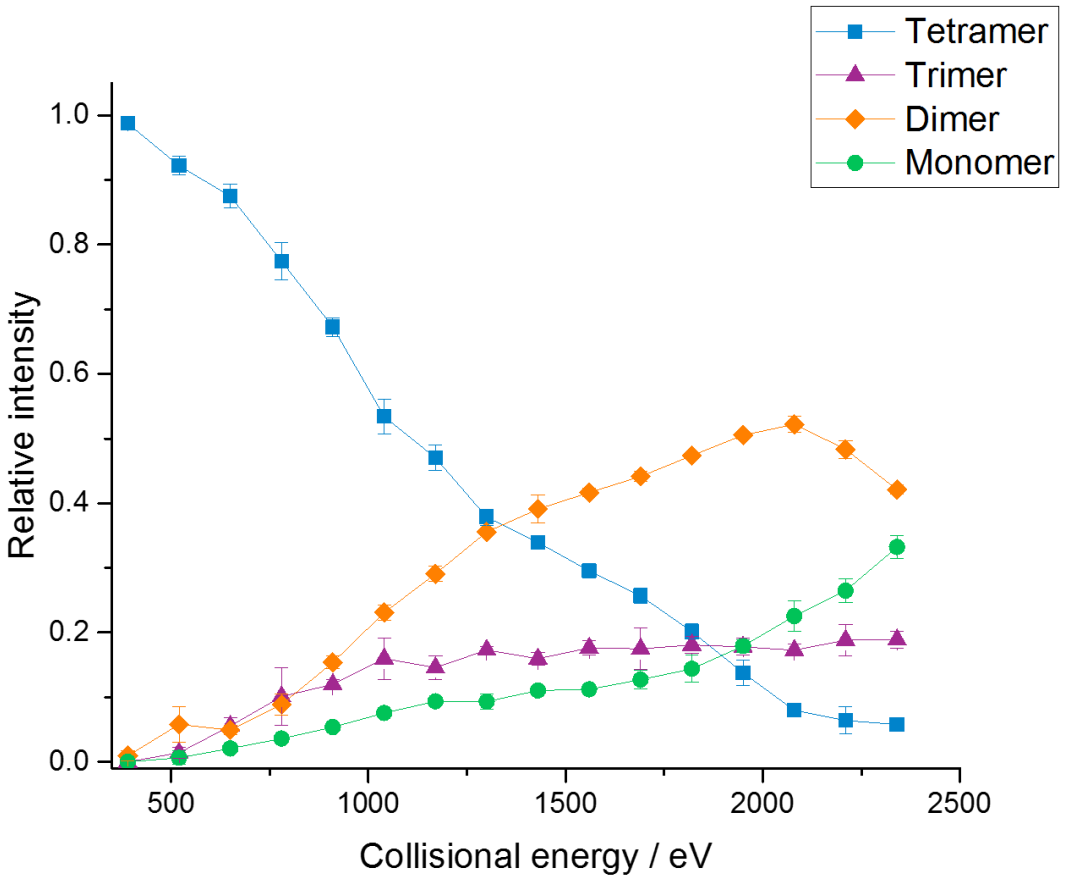

Figure S4: Energy resolved mass spectrometry plot showing the intensity of products produced from the 13+ AqpZ tetramer, as a function of SID energy. Relative intensities are the average of three repeats and error bars represent the standard deviation (*n* = 3).

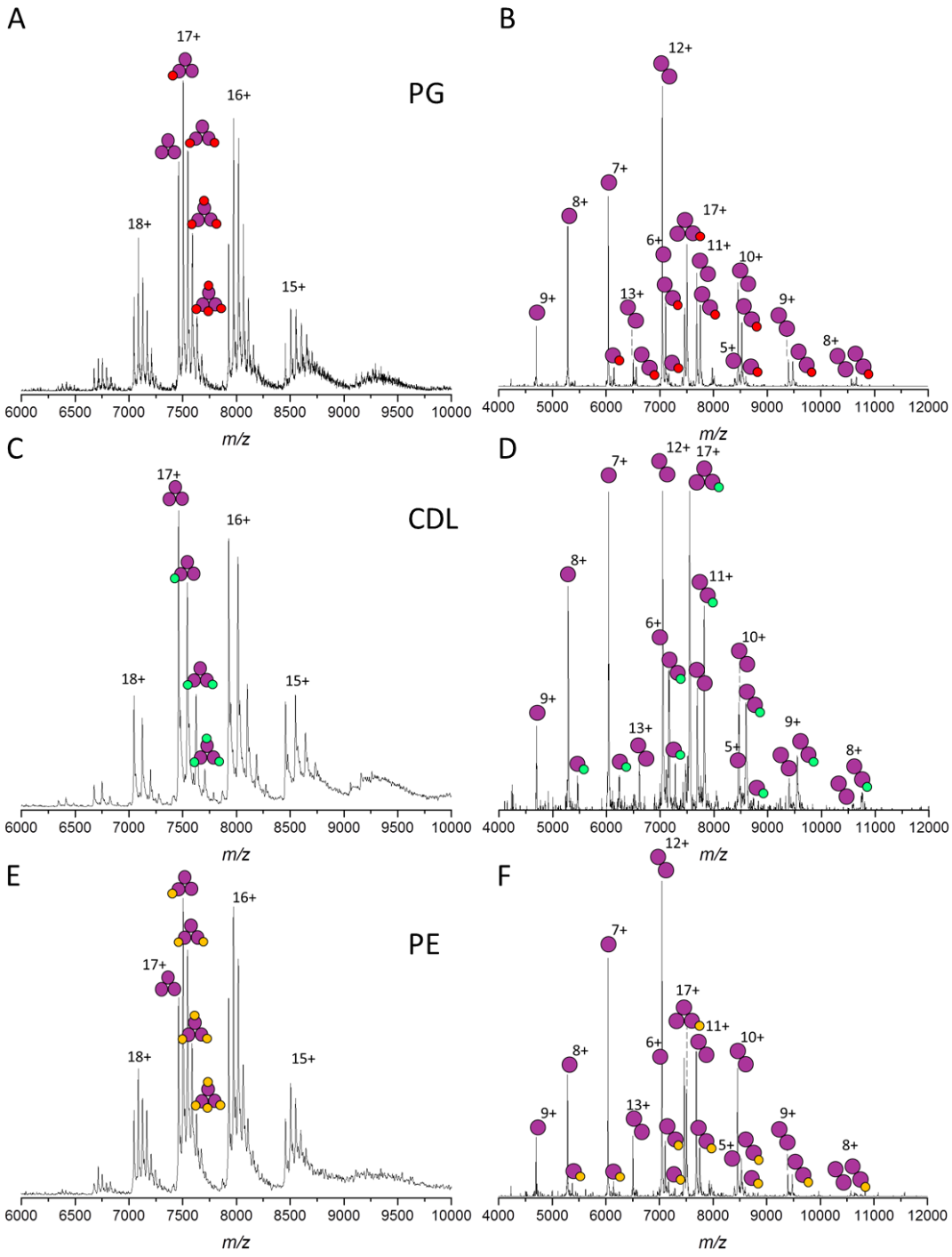

Figure S5: SID of AmtB (purple symbols) bound to PG (red symbols), or CDL (green symbols), or PE (yellow symbols). A) Representative MS spectrum of AmtB mixed with PG. B) SID spectrum for the 17+ AmtB$(PG)_1$ at a collisional energy of 1700 eV. C) Representative MS spectrum of AmtB mixed with CDL. D) SID spectrum for the 17+ AmtB$(CDL)_1$ at a collisional energy of 1700 eV. E) Representative MS spectrum of AmtB mixed with PE. F) SID spectrum for the 17+ AmtB$(PE)_1$ at a collisional energy of 1700 eV.

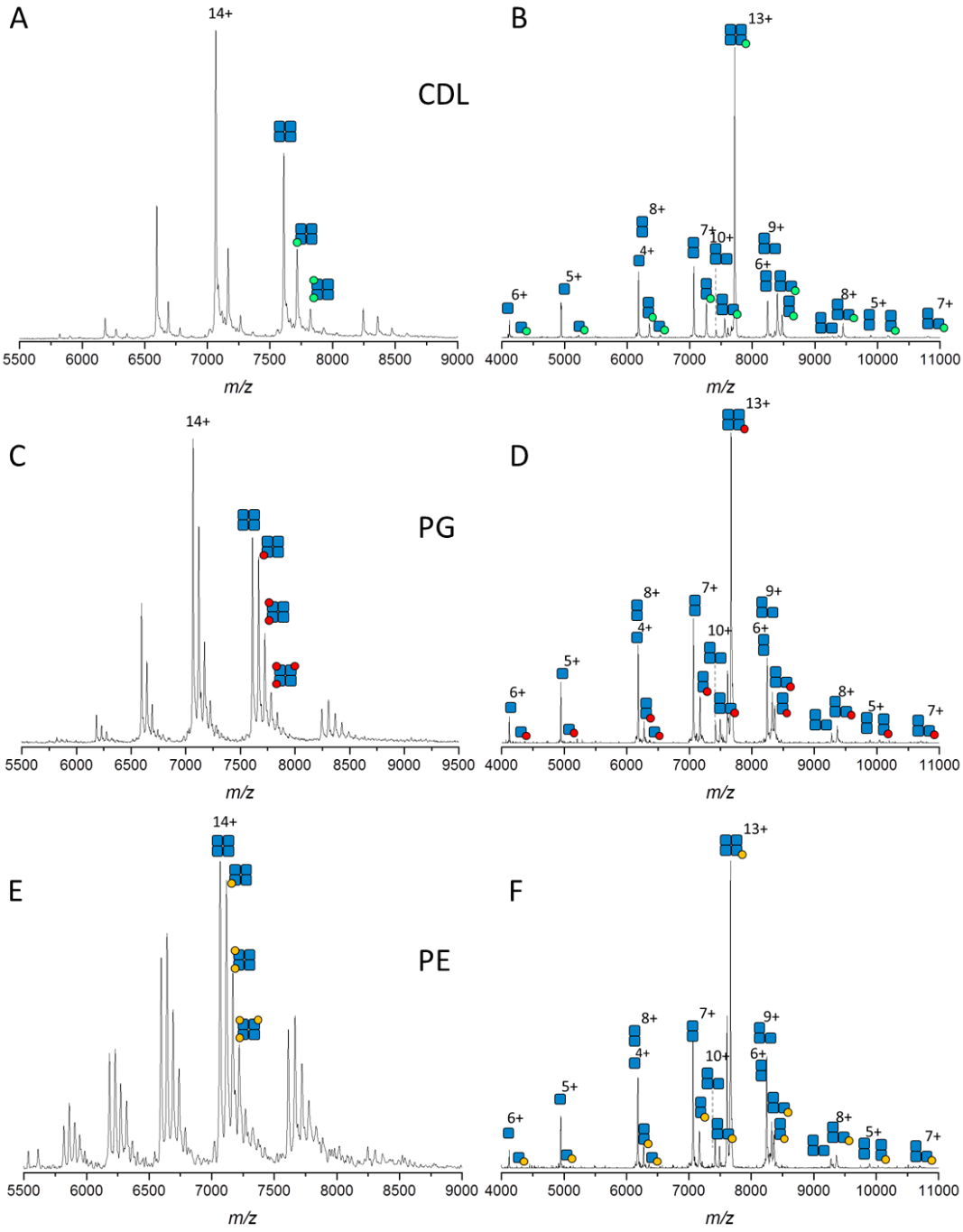

Figure S6: SID of AqpZ (blue symbols) bound to CDL (green symbols), or PG (red symbols), or PE (yellow symbols). A) Representative MS spectrum of AqpZ mixed with CDL. B) SID spectrum for the 13+ AqpZ(CDL)$_1$ at a collisional energy of 1300 eV. C) Representative MS spectrum of AqpZ mixed with PG. D) SID spectrum for the 13+ AqpZ(PG)$_1$ at a collisional energy of 1300 eV. E) Representative MS spectrum of AqpZ mixed with PE. F) SID spectrum for the 13+ AqpZ(PE)$_1$ at a collisional energy of 1300 eV.

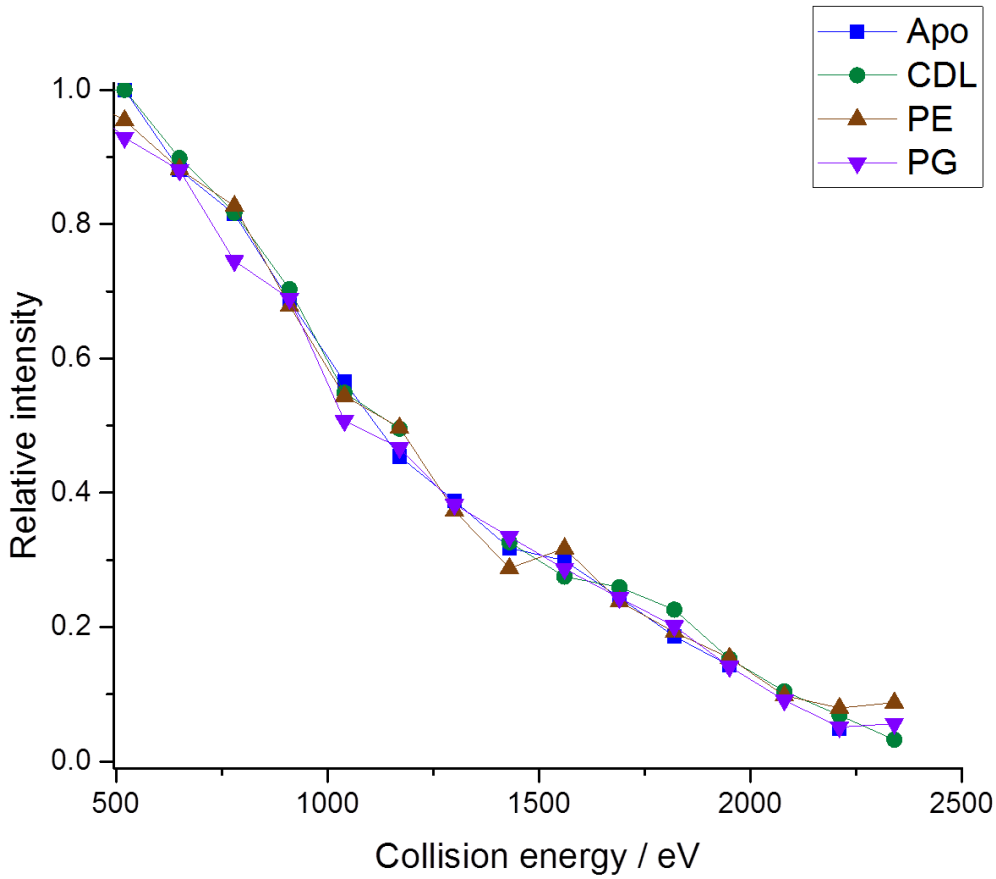

Figure S7: Fragmentation efficiency plot for the 17+ tetrameric *apo* AqpZ, AqpZ$(PG)_1$, AqpZ$(PE)_1$, and AqpZ$(CDL)_1$. The plot shows the decrease in the sum of *(apo* and *holo)* tetramer intensity following surface collision.